Available online at www.sciencedirect.com

SciVerse ScienceDirect

Ceramics International 39 (2013) 5373–5378

CERAMICS INTERNATIONAL

www.elsevier.com/locate/ceramint

Structural and electric properties of polycrystalline $Bi_{1-x}Er_xFeO_3$ ceramics

Haiyang Dai, Zhenping Chen*, Renzhong Xue, Tao Li, Jing Chen, Huiwen Xiang

Department of Technology and Physics, Zhengzhou University of Light Industry, Zhengzhou 450002, China

Received 5 November 2012; received in revised form 12 December 2012; accepted 12 December 2012
Available online 22 December 2012

Abstract

Polycrystalline $Bi_{1-x}Er_xFeO_3$ ceramics were synthesized by the solid state reaction method followed by rapid liquid phase sintering. The effects of Er substitution on the structure, morphology and electrical properties of the $BiFeO_3$ multiferroic ceramics were investigated. X-ray diffraction and Raman studies reveal that the structure of $BiFeO_3$ is changed from rhombohedral to orthorhombic in the Er concentration range of 0.10–0.15, and the impurity phases decrease both due to Er substitution. The X-ray photoelectron spectroscopy shows that Fe^{2+} could be suppressed by Er substitution. The SEM investigations suggest that the Er substitution could significantly reduce the grain sizes and increase the density of the samples. The leakage current is found to be decreased with increasing Er concentration. The dielectric and ferroelectric measurements show that dielectric constant, dielectric loss and ferroelectric properties are strongly dependent on the Er concentration. Er substitution can significantly improve the dielectric constant and remnant polarization, and decrease the dielectric loss by reducing the leakage current.

Keywords: B Spectroscopy; B X-ray methods; C Electrical properties; $Bi_{1-x}Er_xFeO_3$ ceramics

1. Introduction

Multiferroics materials represent a kind of compounds that possess two or three forms of primary ferroic properties: ferroelectricity, ferromagnetism, and ferroelasticity [1–4]. In such materials, magnetization can be induced by the application of electric field and electric polarization can be induced by magnetic field, this phenomenon is also called as the magnetoelectric effect [1–4]. These materials have recently attracted considerable attention due to their potential applications in multifunctional devices, such as information storage, sensors, spintronics memory, transducers, optical filters, magnetic filters and smart devices [1–5]. Besides the potential applications, the theoretical research of multiferroic materials is also fascinating, which enables us understanding the physical origin of the multiferroic properties clearly [3–5]. However, there is a scarcity of materials exhibiting multiferroic behavior. As one of the representative single-phase multiferroic materials, $BiFeO_3$ is known to be the only material that exhibits both ferroelectricity ($T_C \sim 1103$ K) and antiferromagnetism ($T_N \sim 643$ K) above room temperature, which makes it an excellent possible candidate for practical applications at room temperature [1–5].

However, it is difficult to obtain a good polarization hysteresis loop and a large remnant polarization in $BiFeO_3$ due to the high leakage current caused by defects such as impurity phases and oxygen vacancies. Therefore, considerable efforts in research areas have been attempted to improve the properties of $BiFeO_3$ and understand the underlying mechanism [3–9]. Among these methods, partial substitution of Bi^{3+} with La^{3+}, Ho^{3+}, Ba^{2+}, Ca^{2+} and Fe^{3+} with Ni^{2+}, Co^{2+}, Cr^{3+}, Mn^{3+}, Ti^{4+}, and Zr^{4+} in $BiFeO_3$ is proved to be an effective way to improve the physical properties of $BiFeO_3$ [2–5,7–9]. Even though lots of experimental works have been done on rare earth ions substituted bismuth ferrite, there are fewer systematical investigations on Er-substituted $BiFeO_3$ in recent years [9], so the structural and physical properties of Er-substituted $BiFeO_3$ remain unclear. In this paper, $Bi_{1-x}Er_xFeO_3$ ($x=0.00$, 0.05, 0.10, 0.15 and 0.20) samples were synthesized,

*Corresponding author. Tel.: +86 371 63556807; fax: +86 371 63556150.
E-mail address: haiytai@126.com (Z. Chen).

0272-8842/$ - see front matter © 2012 Elsevier Ltd and Techna Group S.r.l. All rights reserved.
http://dx.doi.org/10.1016/j.ceramint.2012.12.043

and the influences of Er substitution at Bi site on the crystal structure, morphology and electrical properties of the $BiFeO_3$ ceramics were investigated.

2. Experimental details

The polycrystalline ceramics samples of $Bi_{1-x}Er_xFeO_3$ ($x=0.00$, 0.05, 0.10, 0.15, and 0.20) were prepared using the solid state reaction method followed by rapid liquid phase sintering. High purity starting powders of Bi_2O_3 (99.999%), Er_2O_3 (99.99%), and Fe_2O_3 (99.99%) were carefully weighed according to the stoichiometric proportions (3% bismuth excess to compensate the Bi loss). These oxides were thoroughly ground in an agate mortar for 6 h using ethanol as a medium to get homogeneous mixture. The mixed powders were dehydrated at 150 °C for 12 h and dry pressed into small discs 11 mm in diameter and 1.6 mm in thickness at 10 MPa pressure. The disks were directly put into a furnace, and then sintered at 850–880 °C with an accuracy of ±1 °C for 30 min. After that they were taken out of the furnace immediately and quenched subsequently to room temperature. To measure the electrical properties of the samples, the disks were carefully polished and Ag electrodes were applied on both surfaces to form metal–insulator–metal capacitors.

The crystal structure of samples was analyzed by X-ray diffraction (XRD, Bruke D8 Adcance) with Cu-Kα radiation. Raman measurements were carried out at room temperature using a Renishaw inVia spectrometer, and the excitation source was the 514.5 nm line of an Ar^+ laser. The valence states of Fe ions were studied by X-ray photoelectron spectroscopy (XPS, PHI Quantera SXM system). The morphologies of the samples were carried out in a scanning electron microscope (SEM, FEI Quanta200). The dielectric measurements were carried out in the frequency range (1 kHz–1 MHz) using an impedance analyzer (Agilent HP 4194 A). The leakage current and ferroelectric properties of $Bi_{1-x}Er_xFeO_3$ ceramics were measured using a ferroelectric tester (RT 6000, Radient Technology, USA) at room temperature.

3. Results and discussion

3.1. X-ray diffraction analysis

The XRD patterns of the $Bi_{1-x}Er_xFeO_3$ ($x=0.00$, 0.05, 0.10, 0.15, and 0.20) ceramics are shown in Fig. 1. A polycrystalline rhombohedral distorted perovskite structure with the space group R3c can be well indexed in the patterns of $x \le 0.10$ samples [8]. A small amount of impurity phases, such as $Bi_2Fe_4O_9$ and $Bi_{25}FeO_{40}$ [2,3], is also detected in the unsubstituted $BiFeO_3$ samples. The intensity of impurity peaks is reduced with the increase in Er^{3+} ions concentration and the impurity peaks almost disappear in $x \ge 0.10$ samples, which show that Er ions can hinder the formation of impurity phases. The reasons may be that the addition of Er can eliminate oxygen vacancies,

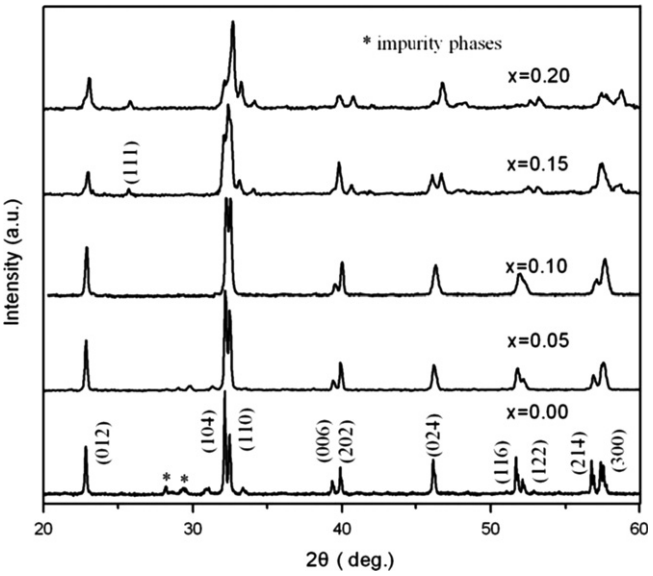

Fig. 1. X-ray diffraction pattern of $Bi_{1-x}Er_xFeO_3$ ceramics ($x=0.00$–0.20).

Table 1
Unit cell parameters and crystal structure of $Bi_{1-x}Er_xFeO_3$ ceramics.

Sample	a (Å)	b (Å)	c (Å)	V (Å^3)	Crystal structure
$x=0.00$	5.57306	5.57306	13.86252	372.87	Rhombohedral
$x=0.05$	5.57248	5.57248	13.75854	370.00	Rhombohedral
$x=0.10$	5.57075	5.57075	13.73486	369.14	Rhombohedral
$x=0.15$	5.61988	5.44223	7.82662	239.37	Orthorhombic
$x=0.20$	5.63815	5.37589	7.57914	229.73	Orthorhombic

avoid compositional fluctuations of Fe^{3+} to Fe^{2+} oxidation, and stabilize the perovskite $BiFeO_3$ phase [1]. In addition, the peaks within 2θ of 20–25° and 30–35° shift to higher angle side when Er concentration x increases from 0.00 to 0.10. The changes indicate that Er^{3+} ions have replaced the Bi^{3+} ions which affected the structure of the original crystals of $BiFeO_3$. However, a structural transition occurs in the Er concentration range of 0.10–0.15, indicated by the appearance of a new (111) peak in the vicinity of $2\theta=27°$and the splitting of the (024) peak around 47° [8]. To determine the structural features of $Bi_{1-x}Er_xFeO_3$ samples, their unit cell parameters were calculated by Jade program (Version 5.0). The lattice parameters, unit cell volume and crystal structure associated with $Bi_{1-x}Er_xFeO_3$ ceramics are shown in Table 1. In the present work, best fits to the measured data are observed using rhombohedral lattice type for $x \le 0.10$ samples and with orthorhombic lattice type for $x \ge 0.15$ samples. Although room temperature phase of $BiFeO_3$ is known to be rhombohedral with R3c space group, the unit cell can also be described in a hexagonal frame of reference [4]. Therefore, in our work, the XRD patterns of $x \le 0.10$ samples were indexed with the space group R3c with a hexagonal unit cell. The refined lattice crystal parameters

are $a=5.57306$ Å, $c=13.86252$ Å for $x=0.00$, which agree well with those of the phase pure $BiFeO_3$ prepared by the solid state reaction method [8], $a=5.57248$ Å, $c=13.75854$ Å for $x=0.05$; $a=5.57075$ Å, $c=13.73486$ Å for $x=0.10$; $a=5.61988$ Å, $b=5.44223$ Å, $c=7.82662$ Å for $x=0.15$; and a=5.63815 Å, $b=5.37589$ Å, $c=7.57914$ Å for $x=0.20$. It can be seen that the values of the parameters a and c decrease slightly with increasing x from 0.00 to 0.10, which result in a slow reduction in volume. While x increases from 0.10 to 0.15, the volume shows a big reduction, indicating that the phase transition from rhombohedral to orthorhombic phase occurs in the Er concentration range of $0.1 \le x \le 0.15$. The changes of the structure of $Bi_{1-x}Er_xFeO_3$ ceramics probably resulted from the smaller ionic radius of Er^{3+} than that of Bi^{3+} [9]. It is very interesting to note that at certain substitution level of Er for $x=0.1$ and 0.15, the system transforms from R3c rhombohedral to orthorhombic phases without the appearance of any other impurity phases.

3.2. Raman analysis

The Raman scattering spectra of the $Bi_{1-x}Er_xFeO_3$ ceramics measured at room temperature are shown in Fig. 2. The frequency range of the Raman scattering spectra is 100–400 cm^{-1}. In the present study, four fundamental Raman modes can be observed in the spectrum of unsubstituted $BiFeO_3$ sample at about 133, 166, 213 and 261 cm^{-1}, which are assigned as A_1-1, A_1-2, A_1-3 and E_1 modes, respectively [10,11]. The mode frequencies are in good agreement with other reports [10–13]. Since Raman scattering spectra are sensitive to atomic displacements, the evolvement of Raman normal modes with increasing Er concentration can provide valuable information about ionic substitution and structure transition of $Bi_{1-x}Er_xFeO_3$ ceramics [12]. As shown in Fig. 2, the A_1-1, A_1-2, A_1-3 and E_1 modes shift gradually toward higher frequencies when Er concentration increases from 0.00 to 0.10, and the mode intensity has a continuous and slow change. The reason for the changes of these modes can be ascribed to the replacement of Bi ions with smaller size and relatively lighter mass Er ions [12,13]. As Er concentration increases from 0.10 to 0.15, the most important feature in the Raman spectra is the disappearance of A_1-2 and A_1-3 modes. At the same time, it can be found that the A_1-1 mode shifts to lower frequencies, while the E_1 mode shifts to higher frequencies and its intensity increases. These phenomena indicate that a structure transition occurs when the Er concentration increases in the range of 0.10–0.15 [12]. The Raman spectrum of $Bi_{0.8}Er_{0.2}FeO_3$ is similar to that of $Bi_{0.85}Er_{0.15}FeO_3$ samples except for a minor upward shift of characteristic peaks position. This means that the $x=0.15$ and 0.20 samples have the same structure. The results of Raman analysis are consistent with the XRD results.

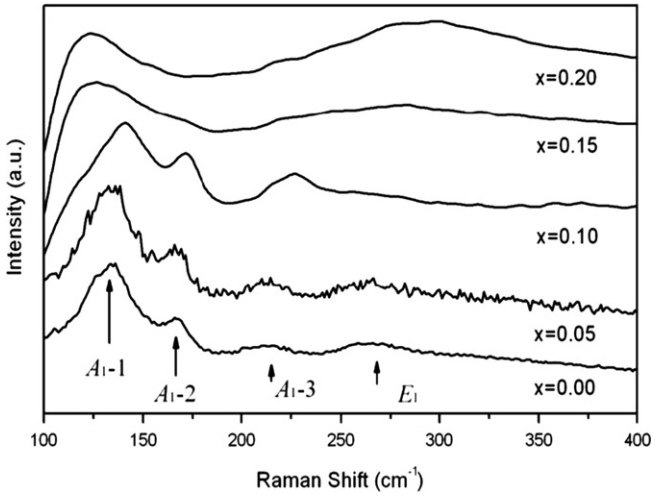

Fig. 2. Raman spectra of $Bi_{1-x}Er_xFeO_3$ samples measured at room temperature.

3.3. XPS analysis

XPS measurements were performed on $Bi_{1-x}Er_xFeO_3$ samples to check the valence states of Fe ions, which affect the multiferroic properties of $BiFeO_3$-based ceramics dramatically [14]. Fig. 3 shows the deconvolution of XPS Fe $2p_{3/2}$ spectrum of unsubstituted $BiFeO_3$ ceramics. One component located at about 709.4 eV corresponds to Fe^{2+}, and the second component located at about 710.8 eV corresponds to Fe^{3+} [14]. The Fe^{2+} to Fe^{3+} ratio is determined by the ratio of the corresponding peak area. The inset of Fig. 3 shows the percentage of Fe^{2+} to the total ions as a function of Er concentration. The percentages of Fe^{2+} to the total ions are 25.3%, 21.5% and 17.5% for $x=0.00$, $x=0.10$ and $x=0.20$ samples, respectively. This means that Fe^{2+} concentration in $Bi_{1-x}Er_xFeO_3$ ceramics decreases with increasing Er concentration. Therefore, Er substitution also can help to suppress the formation of Fe^{2+}. It is well known that

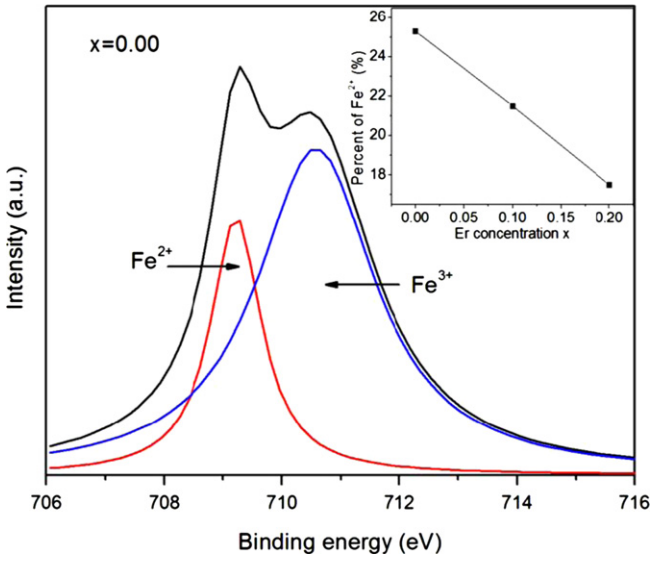

Fig. 3. Deconvolution Fe $2p_{3/2}$ XPS spectrum for unsubstituted $BiFeO_3$ ceramics. The inset shows the percentage of Fe^{2+} as a function of Er concentration.

oxygen vacancies and Fe^{2+} appear simultaneously for charge compensation in $BiFeO_3$-based multiferroic materials [14]. The above results imply that Er substitution can suppress the formation of oxygen vacancies to a certain extent. The reason may be that the strength of Er–O bond (611 kJ/mol) is higher than that of Bi–O bond (343 kJ/mol) [13]; the substitution of Er for Bi in the A site can stabilize the perovskite structure, decrease the volatilization of Bi, and lower the concentration of oxygen vacancies.

3.4. SEM analysis

Fig. 4 presents the surface morphologies of the $Bi_{1-x}Er_xFeO_3$ ceramics for $x=0.00$, 0.10 and 0.20. The unsubstituted $BiFeO_3$ sample has large grain size with a few interstices, while Er-substituted $BiFeO_3$ samples possess smaller grains. The grain size of $Bi_{1-x}Er_xFeO_3$ ceramics decreases monotonically with the increase of Er concentration. It means that the Er substitution at Bi-site reduces significantly the grain size of the $BiFeO_3$ ceramics. The decrease of grain size in the Er-substituted $BiFeO_3$ ceramics can be interpreted by the suppression of oxygen vacancy concentration, which results in slower oxygen ion motion and consequently lowers grain growth rate [15,16]. It also can be seen that, compared with unsubstituted $BiFeO_3$, the Er-substituted $BiFeO_3$ ceramics exhibit denser structure and good homogeneity due to smaller grains.

3.5. Electrical properties

Fig. 5 shows the leakage current density (J) of $Bi_{1-x}Er_xFeO_3$ ceramics as a function of applied electric field (E). It can be seen that all the J–E curves have good symmetry under positive and negative electric fields. Compared to the unsubstituted $BiFeO_3$, the Er-substituted $BiFeO_3$ ceramics show low leakage current density at the same applied electric field. The measured leakage current densities of the $BiFeO_3$, $Bi_{0.95}Er_{0.05}FeO_3$, $Bi_{0.9}Er_{0.1}FeO_3$, $Bi_{0.85}Er_{0.15}FeO_3$ and $Bi_{0.8}Er_{0.2}FeO_3$ ceramics are about 6.8×10^{-5}, 4.7×10^{-5}, 3.4×10^{-5}, 1.5×10^{-5} and 4.2×10^{-6} A/cm^2, respectively, at an applied electric field of 3 kV/cm. It is noted that the values of leakage current get reduced significantly with the increase in the Er concentration x, showing clearly that the leakage current can be effectively reduced by Er substitution. As is well known, the high leakage current in $BiFeO_3$-based materials is caused by oxygen vacancies and iron ions with different valences (Fe^{3+} and Fe^{2+}) induced mainly by Bi volatilization [4]. The oxygen vacancies are trapping centers for electrons, and the electrons they trapped can be readily activated for conduction by the applied electric filed and thus increase the leakage current density of the ceramics [4]. According to the XPS analyses, the oxygen vacancies in $Bi_{1-x}Er_xFeO_3$ ceramics decrease with increasing Er concentration; thus, the leakage current density decreases with increasing Er concentration.

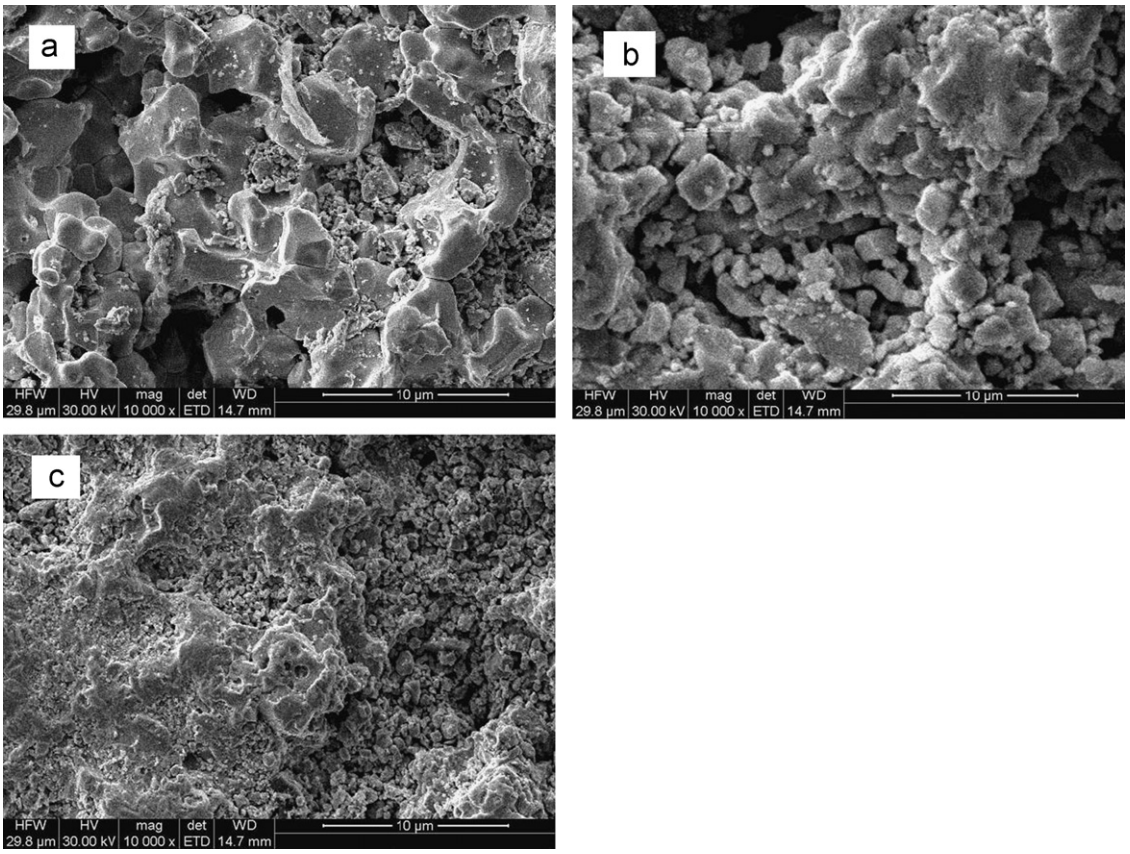

Fig. 4. SEM images of $Bi_{1-x}Er_xFeO_3$ samples: (a) $x=0.00$, (b) $x=0.10$, and (c) $x=0.20$.

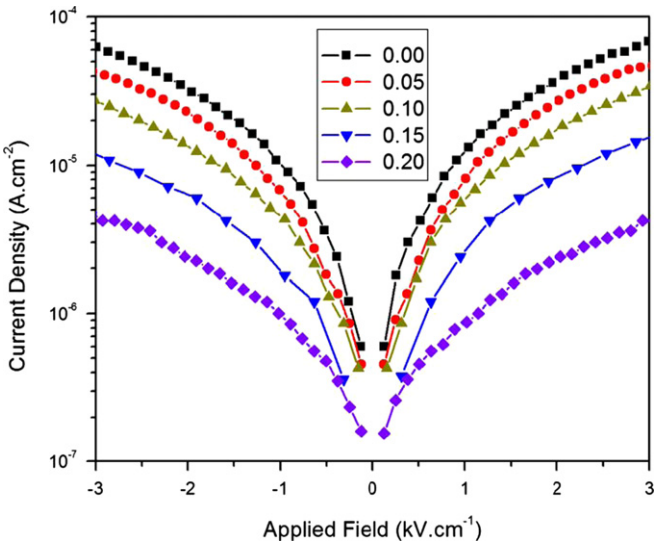

Fig. 5. Leakage current density as a function of applied electrical field in $Bi_{1-x}Er_xFeO_3$ ceramics.

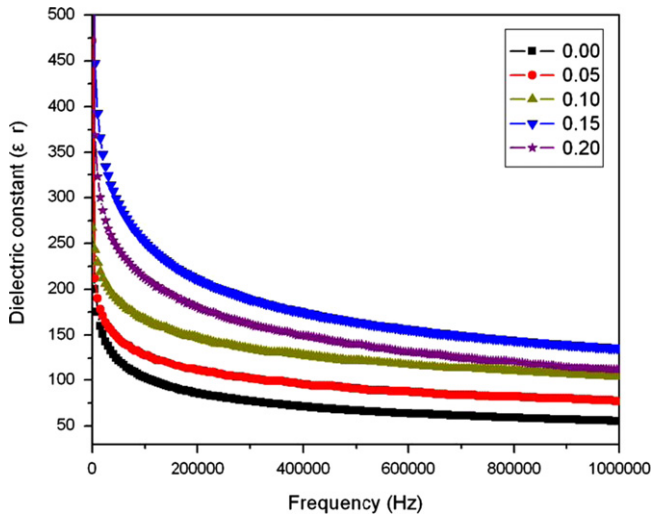

Fig. 6. Dielectric constant of the $Bi_{1-x}Er_xFeO_3$ as a function of frequency.

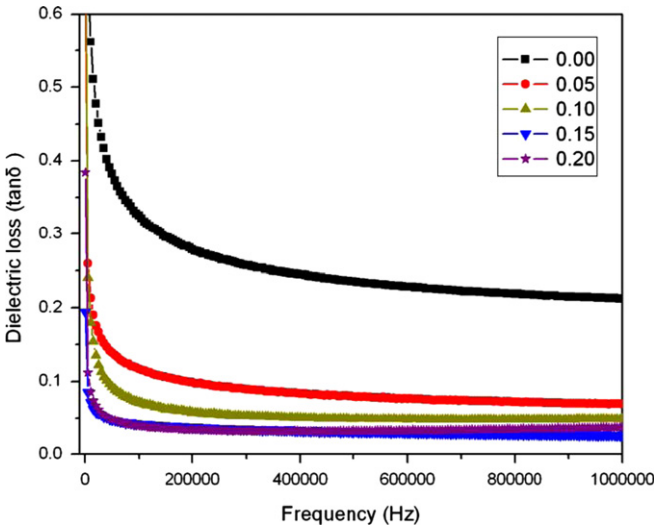

Fig. 7. Dielectric loss of the $Bi_{1-x}Er_xFeO_3$ as a function of frequency.

Fig. 6 shows the dielectric constant (ε_r) of $Bi_{1-x}Er_xFeO_3$ ceramics at room temperature as a function of frequency. The dielectric behaviors of the samples exhibit strong frequency dependence. The value of dielectric constant is high at low frequencies. It decreases rapidly as the frequency increases from 100 to 100 kHz and then decreases slowly and becomes almost constant up to 1 MHz. The observation can be explained by the phenomenon of dipole relaxation wherein at low frequencies the dipoles are able to follow the frequency of the applied field, while they may not have time to build up and undergo relaxation at high frequencies [8]. As shown in Fig. 6, the dielectric constant of Er-substituted $BiFeO_3$ is larger than that of unsubstituted $BiFeO_3$. The dielectric constant of $Bi_{1-x}Er_xFeO_3$ ceramics increases with increasing x from 0.00 to 0.15, then decreases with increasing x from 0.15 to 0.20. The dielectric constant of $Bi_{0.85}Er_{0.15}FeO_3$ (ε_r=136) measured at 1 MHz is about 1.5 times larger than that of unsubstituted $BiFeO_3$ (ε_r=55). This dielectric behavior of $Bi_{1-x}Er_xFeO_3$ ceramics might be understood in terms of oxygen vacancy and the displacement of Fe^{3+} ions. There are always some oxygen vacancies in unsubstituted $BiFeO_3$, which result in relatively high conductivity and small dielectric constant. Substitution of small amount (x=0.0–0.10) of more stable Er^{3+} for Bi^{3+} would stabilize the perovskite structure of $BiFeO_3$ and hence reduce the number of oxygen vacancies and subsequently increase the dielectric constant [17]. Further increase in Er concentration (x=0.15–0.20) would result in a unit cell volume contraction, because the ionic radius of Er^{3+} is smaller than that of Bi^{3+}. The free volume available for the displacement of Fe^{3+} ions in the Fe–O oxygen octahedral becomes smaller and this would lead to a decrease in dielectric polarization [17]. Fig. 7 shows the dielectric loss of $Bi_{1-x}Er_xFeO_3$ ceramics at room temperature as a function of frequency. Similar to the dielectric constant, the dielectric loss also decreases with increasing frequency. The dielectric losses at 1 MHz for x=0.00, 0.05, 0.10, 0.15, and 0.20 samples are about 0.212, 0.069, 0.048, 0.026 and 0.035, respectively. Therefore, substitution of Er into $BiFeO_3$ can effectively inhibit dielectric loss due to the decrease of conductivity in Er-doped samples. It also can be observed that the dielectric loss for Er-substituted samples is rather stable over the entire frequency range investigated, particularly in the frequency range of 10 kHz–1 MHz.

Fig. 8 shows the ferroelectric hysteresis loops for $Bi_{1-x}Er_xFeO_3$ ceramics at room temperature. No fully saturated hysteresis loops could be obtained for all samples at room temperature under the applied field due to high leakage current and partial reversal of polarization. Owing to the different breakdown fields for different samples, various applied electric fields are applied to the samples,

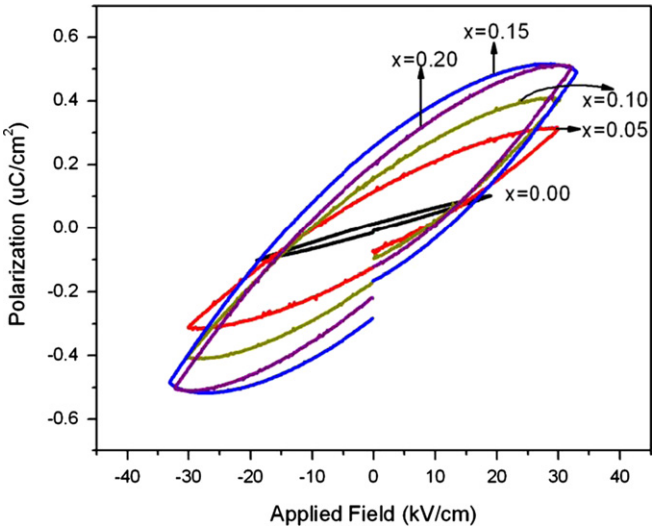

Fig. 8. Ferroelectric hysteresis loops of $Bi_{1-x}Er_xFeO_3$ ceramics at room temperature.

which is about 20 kV/cm for unsubstituted $BiFeO_3$ and about 30 kV/cm for Er-substituted $BiFeO_3$. The values of remnant polarization (P_r) are about 0.014, 0.112, 0.158, 0.258 and 0.201 μC/cm^2 for $x=0.00$, 0.05, 0.10, 0.15 and 0.20 samples, respectively. So the remnant polarization increases with increasing Er concentration from 0.00 to 0.15, while it decreases when Er concentration increases from 0.15 to 0.20. It is striking that substitution of Er^{3+} cation in $BiFeO_3$ can dramatically enhance the ferroelectricity and increase breakdown field.

4. Conclusions

In summary, $Bi_{1-x}Er_xFeO_3$ ceramics with varying x from 0.00 to 0.20 were prepared by the solid state reaction method followed by rapid liquid phase sintering. The influences of Er substitution on the crystal structure, morphology and electrical behaviors of the $BiFeO_3$ were studied. A structure transition from rhombohedral to orthorhombic structure occurs in the Er concentration range of 0.10–0.15, as indicated by XRD and Raman results. Er substitution can suppress the formation of Fe^{2+} and hinder the grain growth of $BiFeO_3$-based ceramics. It is also found that Er substitution can effectively suppress the leakage current and improve the dielectric and ferroelectric properties of $BiFeO_3$-based ceramics. The dielectric constant and remnant polarization for $Bi_{1-x}Er_xFeO_3$ samples increase with increasing Er concentration from 0.00 to 0.15, and decrease with increasing Er concentration from 0.15 to 0.20. The dielectric loss decreases with increasing Er concentration from 0.00 to 0.20.

Acknowledgments

This work is supported by the National Natural Science Foundation of China (Grant no. 11175159) and the School Doctor Foundation of Zhengzhou University of Light Industry (Grant no. 2010BSJJ030).

References

[1] K. Sen, K. Singh, A. Gautam, M. Singh, Dispersion studies of La substitution on dielectric and ferroelectric properties of multiferroic $BiFeO_3$ ceramic, Ceramics International 38 (2012) 243–249.
[2] J. Liu, M.Y. Li, Z.Q. Hu, L. Pei, J. Wang, X.L. Liu, X.Z. Zhao, Effects of ion-doping at different sites on multiferroic properties of $BiFeO_3$ thin films, Applied Physics A 102 (2011) 713–717.
[3] S.K. Pradhan, J. Das, P.P. Rout, V.R. Mohanta, S.K. Das, S. Samantray, D.R. Sahu, J.L. Huang, S. Verma, B.K. Roul, Effect of holmium substitution for the improvement of multiferroic properties of $BiFeO_3$, Journal of Physics and Chemistry of Solids 71 (2010) 1557–1564.
[4] Z.Q. Hu, M.Y. Li, Y. Yu, J. Liu, L. Pei, J. Wang, X.L. Liu, B.F. Yu, X.Z. Zhao, Effects of Nd and high-valence Mn co-doping on the electrical and magnetic properties of multiferroic $BiFeO_3$ ceramics, Solid State Communications 150 (2010) 1088–1091.
[5] A. Kumar, D. Varshney, Crystal structure refinement of $Bi_{1-x}Nd_x$-FeO_3 multiferroic by the Rietveld method, Ceramics International 38 (2012) 3935–3942.
[6] Z.Z. Ma, Z.M. Tian, J.Q. Li, C.H. Wang, S.X. Huo, H.N. Duan, S.L. Yuan, Enhanced polarization and magnetization in multiferroic $(1-x)BiFeO_3$–$xSrTiO_3$ solid solution, Solid State Sciences 13 (2011) 2196–2200.
[7] H. Khelifi, M. Zannen, N. Abdelmoula, D. Mezzane, A. Maalej, H. Khemakhem, M. Es-Souni, Dielectric and magnetic properties of $(1-x)BiFeO_3$–$xBa_{0.8}Sr_{0.2}TiO_3$ ceramics, Ceramics International 38 (2012) 5993–5997.
[8] X.Q. Zhang, Y. Sui, X.J. Wang, Y. Wang, Z. Wang, Effect of Eu substitution on the crystal structure and multiferroic properties of $BiFeO_3$, Journal of Alloys and Compounds 507 (2010) 157–161.
[9] P. Pandit, S. Satapathy, P. Sharma, P.K. Gupta, S.M. Yusuf, V.G. Sathe, Structural, dielectric and multiferroic properties of Er and La substituted $BiFeO_3$ ceramics, Bulletin of Materials Science 34 (2011) 899–905.
[10] P. Rovillain, M. Cazayous, A. Sacuto, D. Lebeugle, D. Colson, Piezoelectric measurements on $BiFeO_3$ single crystal by Raman scattering, Journal of Magnetism and Magnetic Materials 321 (2009) 1699–1701.
[11] A. Gautam, K. Singh, K. Sen, R.K. Kotnala, M. Singh, Crystal structure and magnetic property of Nd doped $BiFeO_3$ nanocrystallites, Materials Letters 65 (2011) 591–594.
[12] V.A. Khomchenko, M. Kopcewicz, A.M.L. Lopes, Y.G. Pogorelov, J.P. Araujo, J.M. Vieira, A.L. Kholkin, Intrinsic nature of the magnetization enhancement in heterovalently doped $Bi_{1-x}A_xFeO_3$ (A=Ca, Sr, Pb, Ba) multiferroics, Journal of Physics D: Applied Physics 41 (2008) 102003-1–102003-4.
[13] J.A. Dean, Lange's Handbook of Chemistry, McGraw-Hill, New York, 1999.
[14] Z. Wen, L. You, X. Shen, X.F. Li, D. Wua, J.L. Wang, A.D. Li, Multiferroic properties of $(Bi_{1-x}Pr_x)(Fe_{0.95}Mn_{0.05})O_3$ thin films, Materials Science and Engineering B 176 (2011) 990–995.
[15] A.Z. Simoes, R.F. Pianno, E.C. Aguiar, E. Longo, J.A. Varela, Effect of niobium dopant on fatigue characteristics of $BiFeO_3$ thin films grown on Pt electrodes, Journal of Alloys and Compounds 479 (2009) 274–279.
[16] G.L. Song, H.X. Zhang, T.X. Wang, H.G. Yang, F.G. Chang, Effect of Sm, Co codoping on the dielectric and magnetoelectric properties of $BiFeO_3$ polycrystalline ceramics, Journal of Magnetism and Magnetic Materials 324 (2012) 2121–2126.
[17] F.G. Chang, G.L. Song, K. Fang, P. Qin, Q.J. Zeng, Effect of gadolinium substitution on dielectric properties of bismuth ferrite, Journal of Rare Earths 24 (2006) 273–276.